Research on the PID Controllers Algorithm of the Quad Rotor

Zhou Hongcheng(✉) and Fang Yuzhuo

School of Electronic and Information Engineering, Jinling Institute of Technology, Nanjing 211169, China
945516882@qq.com

Abstract. In particular affine nonlinear controllers designed using geometric nonlinear control methods, integral backstepping control and backstepping based nonlinear PID controllers have been designed for quad rotor aircraft. A nonlinear simulator was designed to help validate the flight dynamics, aerodynamics models, and controllers developed for quad rotor aircraft. The rotation and translation performance of different nonlinear controllers designed for quad rotor aircraft can be easily verified using simulators in various configurations and subject to interference.

Keywords: Nonlinear control · PID · Flight dynamics · Aerodynamic model · Quad rotor

1 Introduction

Linear controllers offer several advantages for quadrotor aircraft in terms of design information and the availability of control design tools, particularly in relation to robot applications [1]. However, as performance continues to improve and operability becomes a priority, complex control systems are required due to factors such as unpredictable environmental changes, stronger dynamic coupling, and nonlinearity [2]. To address these challenges, there is a need for more sophisticated control systems.

To address the tracking and stability issues of quadcopter aircraft, a nonlinear controller was designed. Additionally, a 3D graphic animation was implemented in the simulator to visualize the behavior of the quad rotor, as shown in Fig. 1. The response of a quad rotor in terms of attitude, position, and altitude can be obtained along the 3D path of the quad rotor.

X. Chen et al. (Eds.): IoTaaS 2023, LNICST 585, pp. 143–151, 2025.
https://doi.org/10.1007/978-3-031-70507-6_12

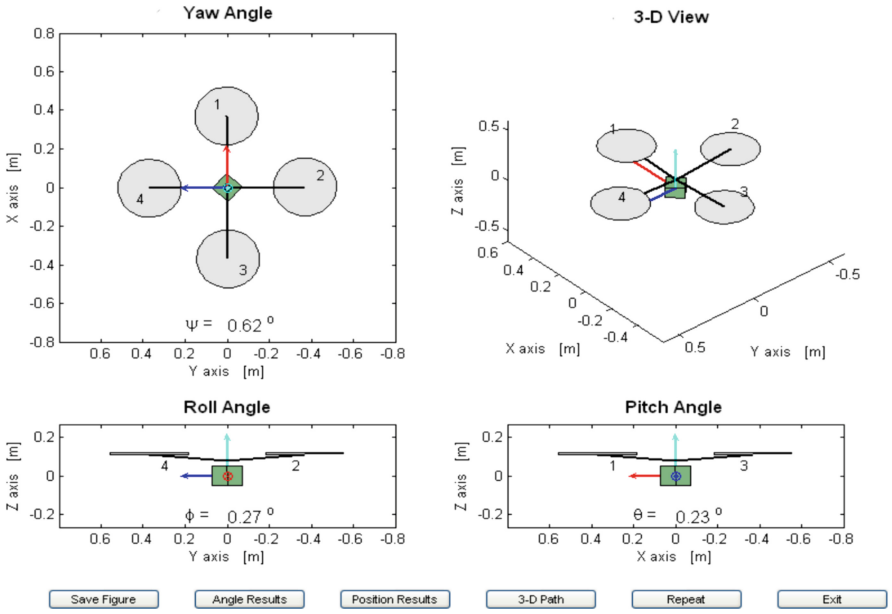

Fig. 1. Quad rotor simulator.

We recall derived nonlinear model for translational and rotational quad rotor aircraft,

$$f(x,u)_{translational} = \begin{pmatrix} \dot{x} \\ \dfrac{(\cos\phi \sin\theta \cos\psi + \sin\phi \sin\psi)}{m} u_1 \\ \dot{y} \\ \dfrac{(\cos\phi \sin\theta \sin\psi - \sin\phi \cos\psi)}{m} u_1 \\ \dot{z} \\ -g + \dfrac{(\cos\phi \cos\theta)}{m} u_1 \end{pmatrix} \tag{1}$$

$$f(x,u)_{rotational} = \begin{pmatrix} \dot{\phi} \\ \dot{\theta}\dot{\psi}\left(\dfrac{J_y - J_z}{J_x}\right) + \dfrac{l}{J_x} u_2 \\ \dot{\theta} \\ \dot{\phi}\dot{\psi}\left(\dfrac{J_z - J_x}{J_y}\right) + \dfrac{l}{J_y} u_3 \\ \dot{\psi} \\ \dot{\phi}\dot{\theta}\left(\dfrac{J_x - J_y}{J_z}\right) + \dfrac{1}{J_z} u_4 \end{pmatrix} \tag{2}$$

where x represents the states and u the inputs to the quad rotor aircraft. The inputs to quad rotor are defined as, vertical force input u_1, roll actuator input u_2, pitch actuator input u_3 and yaw moment input u_4 given by [3],

$$\left.\begin{aligned} u_1 &= b(\Omega_1^2 + \Omega_2^2 + \Omega_3^2 + \Omega_4^2) \\ u_2 &= b(\Omega_4^2 - \Omega_2^2) \\ u_3 &= b(\Omega_3^2 - \Omega_1^2) \\ u_4 &= d(\Omega_2^2 + \Omega_4^2 - \Omega_1^2 - \Omega_3^2) \end{aligned}\right\} \tag{3}$$

The coefficients of thrust b and resistance d are respectively represented in the equation. The control strategy used to stabilize the quadcopter aircraft uses priority rules to sequentially adjust each state [4]. The height of the quad rotor is controlled by vertical force input u_1, and the required roll and pitch angles for the quadcopter are extracted from the translation subsystem. The rotation controller controls the input u_2, u_3, u_4 and stabilizes the quad rotor.

2 Rotational Control

If there is a nonlinear feedback control law that converts the system into an adjoint form of coordinate transformation and eliminates nonlinear dynamics, then the nonlinear control system (4) is feedback linearizable, simplifying the original system into a linearly controllable system [5].

The dimension vector field $f_1(x), f_2(x), \ldots, f_k(x)$ defined on the open subset D_0. A mapping which is each point x of D_0 is assigned a dimension vector.

Definition 1 The dimensional distribution on D_0 is a mapping that assigns a dimensional subspace $\Delta(x)$ to each D_0, such that there exists a satisfying $k-$ dimensional vector field $f_1(x), f_2(x), \ldots, f_k(x)$,

Let $[f_i, f_j]$ denote the Lie bracket,

$$[f_i, f_j] = ad_{f_i} f_j \triangleq \frac{\partial f_j}{\partial x} f_i - \frac{\partial f_i}{\partial x} f_j \tag{4}$$

$$ad_{f_i}^k f_{\mathbf{j}} = ad_{f_i} ad_{f_i}^{k-1} f_{\mathbf{j}} \; \mathrm{ad}_{\mathrm{f_r}}^0 f_{\mathbf{j}} = f_{\mathbf{j}} \tag{5}$$

$$f(x) = \left[x_2 \;\; (x_4 x_6)\left(\tfrac{J_y - J_z}{J_x}\right) \;\; x_4 \;\; (x_2 x_6)\left(\tfrac{J_z - J_x}{J_y}\right) \;\; x_6 \;\; (x_2 x_4)\left(\frac{J_x - J_y}{J_z}\right) \right]^T \tag{6}$$

$$g_1(x) = \left[0 \;\; \tfrac{l}{J_x} \;\; 0 \;\; 0 \;\; 0 \;\; 0 \right]^T \tag{7}$$

$$g_2(x) = \left[0 \;\; 0 \;\; 0 \;\; \tfrac{l}{J_y} \;\; 0 \;\; 0 \right]^T \tag{8}$$

$$g_3(x) = \left[0 \;\; 0 \;\; 0 \;\; 0 \;\; 0 \;\; \tfrac{1}{J_z} \right]^T \tag{9}$$

$$y = \begin{bmatrix} x_1 \; x_3 \; x_5 \end{bmatrix}^T \tag{10}$$

Let us check the distribution $\Delta(x)$ for involutivity.

$$\Delta_0(x) = span\{g_1(x), g_2(x), g_3(x)\} = span\left\{ \begin{bmatrix} 0 \\ l/J_x \\ 0 \\ 0 \\ 0 \\ 0 \end{bmatrix}, \begin{bmatrix} 0 \\ 0 \\ 0 \\ l/J_y \\ 0 \\ 0 \end{bmatrix}, \begin{bmatrix} 0 \\ 0 \\ 0 \\ 0 \\ 0 \\ 1/J_z \end{bmatrix} \right\} \tag{11}$$

$$\Delta_1(x) = span\left\{g_1(x), g_2(x), g_3(x), ad_f g_1(x), ad_f g_2(x), ad_f g_3(x)\right\} \tag{12}$$

$$ad_f g_1(x) = -\left[l/J_x \; 0 \; 0 \; \frac{x_6 l}{J_x}\left[\frac{J_z - J_x}{J_y}\right] \; 0 \; \frac{x_4 l}{J_x}\left[\frac{J_x - J_y}{J_z}\right] \right]^T \tag{13}$$

$$ad_f g_2(x) = -\left[0 \; \frac{x_6 l}{J_y}\left[\frac{J_y - J_z}{J_x}\right] \; l/J_y \; 0 \; 0 \; \frac{x_2 l}{J_y}\left[\frac{J_x - J_y}{J_z}\right] \right]^T \tag{14}$$

$$ad_f g_3(x) = -\left[0 \; \frac{x_4}{J_z}\left[\frac{J_y - J_z}{J_x}\right] \; 0 \; \frac{x_6}{J_z}\left[\frac{J_z - J_x}{J_y}\right] \; 1/J_z \; 0 \right]^T \tag{15}$$

Since the matrices in expressions (12) and (13) have equal rank values, the new vector field obtained by performing a lie bracket operation on two arbitrary vector fields from the original vector field k (i.e. evaluating the derivative of one vector field k along another vector field) is not linearly independent, but linearly related to the previous vector field. In other words, the new vector field remains in the original span space of the vector field and does not form a new direction [8].

The vector field $ad_f g_1$ along g_1 was obtained. The rank of the augmented matrix remains equal to the rank of the original matrix. Therefore, $\Delta_o(x)$ is involutive. All conditions are met, and the affine nonlinear system is feedback linearized. Furthermore, the sum of the two vector fields f and g in the parentheses indicates that the quad rotor of the rotating subsystem is completely controllable.

Secondly, the relative degree of the rotating subsystem was studied. Two conditions were found to be met. For the nonlinear system (10), we take into account the nonlinear coordinate transformation. Nonlinear coordinate transformation can be described as,

$$Z = \Phi(x) \tag{16}$$

where Z and X were vectors of equal dimensions, Φ was nonlinear vector functions,

$$\begin{aligned} Z_{\mathbf{1}} &= \phi_1(x_1, x_2, \cdots, x_n) \\ Z_2 &= \phi_2(x_1, x_2, \cdots, x_n) \\ &\vdots \\ Z_n &= \phi_n(x_1, x_2, \cdots, x_n) \end{aligned} \tag{17}$$

The first condition for nonlinear coordinate transformation is that its inverse transformation exists and is single valued,

$$X = \Phi^{-1}(Z) \tag{18}$$

The second condition is that both $\Phi(X)$ and $\Phi^{-1}(Z)$ are smooth vector fields, that is, the functions of both Φ and Φ^{-1} have continuous partial derivatives of any order. In short, the first condition is reversible, and the second condition is differentiable [9].

The diffeomorphism $\boldsymbol{\zeta} = (\zeta_1, \zeta_2, \zeta_3, \zeta_4, \zeta_5, \zeta_6) = \varsigma_F(x)$ that transforms (10) to a linear controllable system can be obtained by solving the partial differential equations,

$$L_{g_1} h_1(x) = 0, L_{g_2} h_2(x) = 0, L_{g_3} h_3(x) = 0$$

For $\Delta_o(x)$, due to its involution, the Frobenius theorem guarantees the existence of solutions.

$$\begin{aligned} \zeta_1 &= h_1(x) = x_1,\ \zeta_2 = L_f h_1(x) = x_2 \\ \zeta_3 &= h_2(x) = x_3,\ \zeta_4 = L_f h_2(x) = x_4 \\ \zeta_5 &= h_3(x) = x_5,\ \zeta_6 = L_f h_3(x) = x_6 \end{aligned} \tag{19}$$

Therefore, differential homeomorphism $\boldsymbol{\zeta} = \varsigma_F(x) = (x_1, x_2, x_3, x_4, x_5, x_6)$ is globally defined in $D_0 \to \Re^6$. Then $w = \begin{pmatrix} w_1 & w_2 & w_3 \end{pmatrix}^T$ can be transformed into Brunovsky form by definition,

$$w_i^{(r_i)} = L_f^{r_i} h_i + \sum_{j=1}^{m} L_{g_j} L_f^{r_i - 1} h_i u_j \tag{20}$$

In our case, $i = (1, 2, 3)$ and $m = (1, 2, 3)$ with $L_{g_j} L_f^{r_i - 1} h_i(x) \neq 0$ for at least one j.A routine calculation shows that,

$$w_1 = \left[x_4 x_6 \left(\frac{J_y - J_z}{J_x} \right) + \frac{l}{J_x} u_1 \right] \tag{21}$$

$$w_2 = \left[x_2 x_6 \left(\frac{J_z - J_x}{J_y} \right) + \frac{l}{J_y} u_2 \right] \tag{22}$$

$$w_3 = \left[x_2 x_4 \left(\frac{J_x - J_y}{J_z} \right) + \frac{1}{J_z} u_3 \right] \tag{23}$$

From (21), (22) and (23),

$$\begin{bmatrix} w_1 \\ w_2 \\ w_3 \end{bmatrix} = \begin{bmatrix} x_4 x_6 \left(\frac{J_y - J_z}{J_x} \right) \\ x_2 x_6 \left(\frac{J_z - J_x}{J_y} \right) \\ x_2 x_4 \left(\frac{J_x - J_y}{J_z} \right) \end{bmatrix} + E \begin{bmatrix} u_1 \\ u_2 \\ u_3 \end{bmatrix} \tag{24}$$

or,

$$\begin{bmatrix} u_1 \\ u_2 \\ u_3 \end{bmatrix} = E^{-1} \left(\begin{bmatrix} w_1 \\ w_2 \\ w_3 \end{bmatrix} - \begin{bmatrix} x_4 x_6 \left(\frac{J_y - J_z}{J_x} \right) \\ x_2 x_6 \left(\frac{J_z - J_x}{J_y} \right) \\ x_2 x_4 \left(\frac{J_x - J_y}{J_z} \right) \end{bmatrix} \right) \tag{25}$$

where E is a decoupling square matrix defined obviously.

Therefore, using differential equations $\boldsymbol{\zeta} = \varsigma_F(x)$ substituting (25) into (10) to obtain the form,

$$\dot{\zeta} = \begin{bmatrix} 1\,0\,0\,0\,0\,0 \\ 0\,0\,0\,0\,0\,0 \\ 0\,0\,1\,0\,0\,0 \\ 0\,0\,0\,0\,0\,0 \\ 0\,0\,0\,0\,1\,0 \\ 0\,0\,0\,0\,0\,0 \end{bmatrix} \boldsymbol{\zeta} + \begin{bmatrix} 1\,0\,0 \\ 0\,0\,0 \\ 0\,1\,0 \\ 0\,0\,0 \\ 0\,0\,1 \\ 0\,0\,0 \end{bmatrix} \begin{bmatrix} w_1 \\ w_2 \\ w_3 \end{bmatrix} \tag{26}$$

Any stable linear control law (26) can be used to stabilize the original system (10) by performing inverse $x = \varsigma_F^{-1}(\boldsymbol{\zeta})$ and control transformations given in (26). The control law (25) with a linear controller asymptotically stabilizes the attitude angles of the quad rotor aircraft. In addition, stability is global on D because $x = \varsigma_F^{-1}(\boldsymbol{\zeta})$ is a differential homeomorphism on D, and the control law (25) is well defined on D [10].

3 Nonlinear Simulation Results

The angle and its time derivative of the rotating subsystem are not dependent on the translation component, as can be clearly seen from the 6-DOF equation of a quad rotor aircraft. However, the conversion depends on the angle. Ideally, it can be imagined as two subsystems, angular rotation and linear translation. Due to the complete independence of the angular rotation subsystem from other subsystems, adjustments have been made to it [13].

The rotation control maintains the 3D direction of the quadcopter at the desired value. The roll and pitch angles are usually forced to zero, allowing hovering flight. The task of the rotation controller is to compensate for initial errors, stabilize roll angle, pitch angle, and yaw angle, and maintain them at zero. This is achieved using a nonlinear control law u_2, u_3 and u_4.

Let's use a nonlinear controller to simulate a closed-loop system. We summarize the different system parameters of quad rotor used in nonlinear simulations in Table 1.

The initial conditions used are $\phi = \theta = 0.5$ rad, $\dot{\phi} = \dot{\theta} = 0.5$ rad/sec, $Z = 1$ meters. For the controller, the reference inputs are $Z_d = 1, \dot{x}_d = \dot{y}_d = 0, \psi_d = 0$.

Since the prototype system has some delays because of RS232 communications and actuators dynamics and actuator saturation problem. As a solution to address the

Table 1. Physical parameters of quad rotor

Parameter	Value	Unit
l	0.3	m
J_x	0.0154	$kg \cdot m^2$
J_y	0.0154	$kg \cdot m^2$
J_z	0.0309	$kg \cdot m^2$
m	0.6	kg

delays caused by RS232 communications and actuator dynamics, two Simulink discrete step delay blocks were implemented in the feedback loop and actuator. Furthermore, considering the maximum angular speed of the motor, which is 650 rad/sec, a saturation block was strategically positioned between the controller and the delay block. Altitude data is provided at 20Hz (as on the SFR sensor). Angles data and angular rates are provided at 100Hz max. Simulation is also done at 100Hz. The added noise and delay are reasonably close to the reality.

It shows the response of the attitude nonlinear controller to a stable quad aircraft in Fig. 2. The simulation results in Fig. 2 were obtained using the dynamic model of the actuator. From the attitude response of the quad rotor, it can be seen that the controller effectively stabilized the roll angle, pitch angle, and yaw angle in less than 6 s.

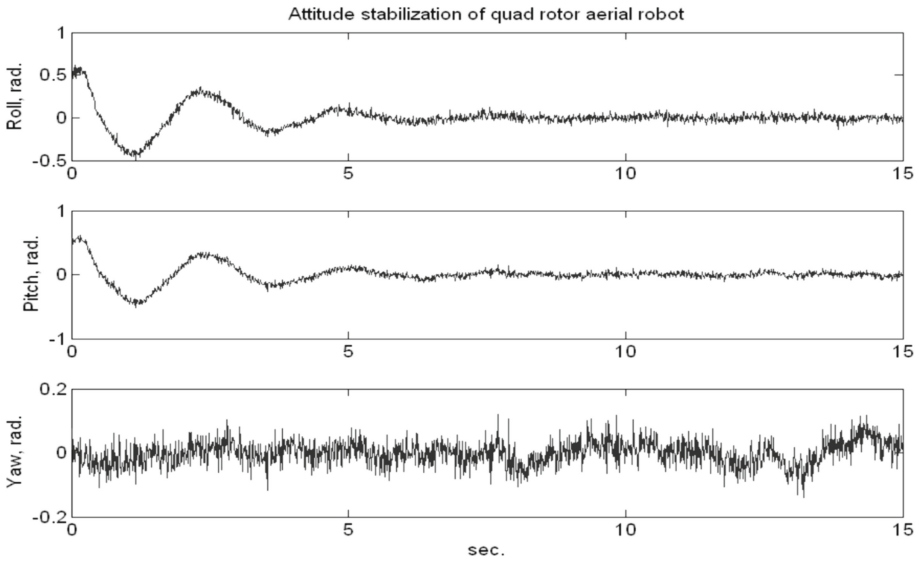

Fig. 2. Attitude response of quad rotor

Figure 3 presents the altitude and position response of a quad rotor aircraft. The results depicted in Fig. 3 demonstrate the effectiveness of the position controller in successfully maintaining the quad's attitude at a specified point.

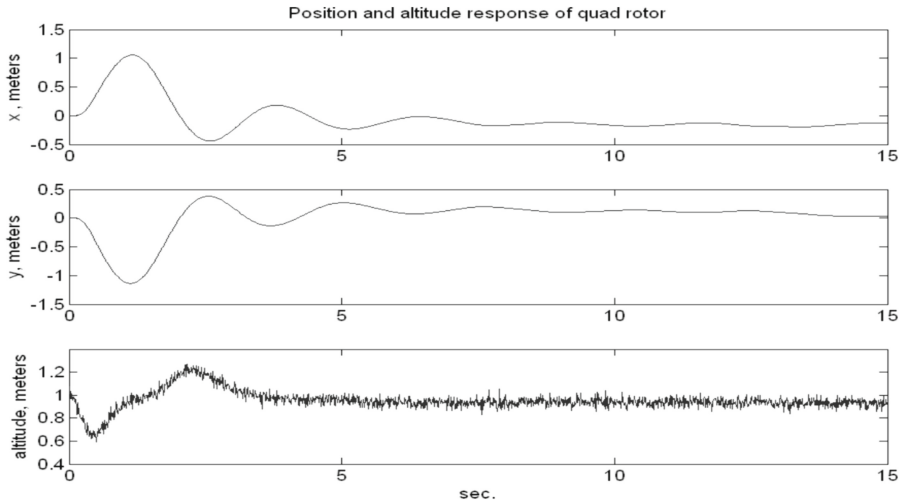

Fig. 3. Position and altitude response of quad rotor

The nonlinear simulation results provide evidence of the effective control achieved by the nonlinear controller for the quad rotor aircraft. In contrast to traditional Jacobian linearization, the feedback linearization employed in this study utilizes an accurate feedback linearization of the rotating subsystems rather than a Taylor series extension. This approach involves transforming the nonlinear dynamics into a linearized form through the application of state feedback and input state linearization techniques. However, it is important to note that feedback linearization does have certain limitations. The presence of parameter uncertainty or unmodeled dynamics can compromise its robustness. This is due to the unavailability of an exact model of the nonlinear system during the feedback linearization process.

4 Conclusion

Three different nonlinear control strategies for full control of quad rotor aircraft are presented. The first technique employed in this study utilizes affine nonlinear control methods, incorporating geometric approaches to nonlinear control. The stabilization and tracking performance with affine nonlinear controller is presented which seems to be quite good. Global asymptotic stability of the designed nonlinear controller is proved. However, it is important to note that the presence of parameter uncertainty or unmodeled dynamics poses a challenge to ensuring robustness. This limitation arises from the unavailability of an exact model of the nonlinear system during the process of feedback linearization.

Acknowledgment. This work was supported by Cooperative Project of Jiangsu Province production, teaching and research (No. BY2021381), Jin Ling Institute of Technology Ph. D. Startup Fund(jit-b-202314).

References

1. Ma, L., Zhu, F., Zhang, J., Zhao, X.: Leader-follower asymptotic consensus control of multi-agent systems: an observer-based disturbance reconstruction approach. IEEE Trans. Cybern. **53**, 1311 (2021)
2. Wu, G., Chen, G., Zhang, H., Huang, C.: Fully distributed event-triggered vehicular platooning with actuator uncertainties. IEEE Trans. Veh. Technol. **70**(7), 6601–6612 (2021)
3. Tang, Y., Zhang, D., Shi, P., Zhang, W., Qian, F.: Event-based formation control for nonlinear multiagent systems under dos attacks. IEEE Trans. Autom. Control **66**(1), 452–459 (2021)
4. Zhao, G., Hua, C.: Leader-following consensus of multiagent systems via asynchronous sampled-data control: a hybrid system approach. IEEE Trans. Autom. Control **67**(5), 2568–2575 (2022)
5. Wei, C., Gui, M., Zhang, C., Liao, Y., Dai, M.Z., Luo, B.: Adaptive appointed-time consensus control of networked euler lagrange systems with connectivity preservation. IEEE Trans. Cybern. **52**(11), 12379 (2021)
6. Zhao, L., Chen, X., Yu, J., Shi, P.: Output feedback-based neural adaptive finitetime containment control of non-strict feedback nonlinear multi-agent systems, IEEE Trans. Circuits Syst. I Regul. Pap. **69**(2), 847–858 (2022)
7. Jiang, D., Wen, G., Peng, Z., Huang, T., Rahmani, A.: Fully distributed dual-terminal event-triggered bipartite output containment control of heterogeneous systems under actuator faults. IEEE Trans. Syst. Man Cybern. Syst. **52**, 5518 (2021)
8. Cheng, F., Liang, H., Wang, H., Zong, G., Xu, N.: Adaptive neural self-triggered bipartite fault-tolerant control for nonlinear mass with dead-zone constraints. IEEE Trans. Autom. Sci. Eng. **20**(3), 1663 (2022)
9. Zhang, H., Zhao, X., Zong, G., Xu, N.: Fully distributed consensus of switched heterogeneous nonlinear multi-agent systems with hysteresis input. IEEE Trans. Netw. Sci. Eng. **9**(6), 4198–4208 (2022)
10. Yan, C., Zhang, W., Su, H., Li, X.: Adaptive bipartite time-varying output formation control for multiagent systems on signed directed graphs. IEEE Trans. Cybern. **9**, 1–14 (2021)
11. Cai, Y., Zhang, H., Wang, Y., Gao, Z., He, Q.: Adaptive bipartite fixed-time varying output formation-containment tracking of heterogeneous linear multiagent systems. IEEE Trans. Neural Networks Learn. Syst. **9**, 1–11 (2021)
12. Luo, Y., Zhu, W., Cao, J., Rutkowski, L.: Event-triggered finite-time guaranteed cost h-infinity consensus for nonlinear uncertain multi-agent systems. IEEE Trans. Network Sci. Eng. **9**(3), 1527–1539 (2022)
13. Yu, J., Dong, X., Li, Q., Ren, L.J.Z.: Fully adaptive practical time-varying output formation tracking for high-order nonlinear stochastic multiagent system with multiple leaders. IEEE Trans. Cybern. **51**(4), 2265–2277 (2021)